

An optically thick inner corona geometry for the Very High State Galactic Black Hole XTE J1550–564

Chris Done¹ and Aya Kubota²

¹*Department of Physics, University of Durham, South Road, Durham DH1 3LE, UK; chris.done@durham.ac.uk*

²*Cosmic Radiation Laboratory, Institute of Physical and Chemical Research, 2-1 Hirosawa, Wako-shi, Saitama, 351-0198, Japan; aya@crab.riken.jp*

Accepted 2005 * **. Received 2005 * **, in original form 2005 * **

ABSTRACT

We investigate the accretion disc structure in the strongly Comptonised spectra seen at high luminosities from galactic black holes (variously termed the very high or steep power law dominant state). We use simultaneous ASCA-RXTE data on two such spectra from the black hole transient XTE J1550-564 to constrain the disc and Comptonized luminosity. The broad bandpass of the data gives robust estimates of the disc temperature and luminosity despite the strong Comptonisation distorting the spectrum. The disc temperature is much lower than that seen from the same source at the same luminosity in its disc dominated spectra (high/soft or thermal dominant state). This implies that the disc emissivity or/and the disc area has changed between the two states. We build a spectral model of a Comptonising corona over an inner disc to show explicitly that a standard disc emissivity requires a large increase in inner disc radius for the very high state spectra. While such models can describe the spectra, it seems more probable that the disc emissivity *changes* in the presence of the corona. We build a specific model of an inner corona which is coupled energetically to the disc, in which some fraction f of the accretion power is dissipated in the corona leaving only a fraction $1 - f$ to be dissipated in the optically thick disc (Svensson & Zdziarski 1994). We show that this can explain the low temperature/high luminosity disc emission seen in the very high state with only a small increase in radius of the disc. While the inferred disc truncation is probably not significant given the model uncertainties, it is consistent with the low frequency QPO and gives continuity of properties with the low/hard state spectra. Irrespective of such details, there is clear evidence in the very high state spectra that the growth of the corona affects the disc, strongly favouring models in which the corona is part of the same accretion flow structure as gives rise to the disc.

Key words:

accretion, accretion discs – black hole physics – radiation mechanisms: thermal – radiative transfer – X-rays: binaries – X-rays: individual: XTE J1550 – 564

1 INTRODUCTION

Galactic black hole binaries at high mass accretion rates show spectra which are often dominated by a soft, quasi-thermal component (e.g. the review by Tanaka & Lewin 1995). This shape matches very well with that expected from an optically thick, geometrically thin accretion disc, as described in the seminal paper by Shakura & Sunyaev (1973). This identification is strengthened by observations of variability in which the temperature and luminosity of this quasi-thermal component change together in such a way as

to indicate that the size of the emitting structure remains approximately constant. The last stable orbit is the only obvious candidate for such a radius, so this gives compelling evidence for a key prediction of general relativity, as well as providing an observable diagnostic of the mass and spin of the black hole (Ebisawa et al 1994; Kubota et al 2001; Gierlinski & Done 2004; Kubota & Done 2004; hereafter KD04). The most recent models of accretion disc spectra are able to reproduce this behaviour, giving theoretical underpinning to the observations (Davis et al 2005).

The disc dominated spectra always contain some small

fraction of emission in a tail extending to much higher energies. However, some high luminosity spectra have a rather different spectral shape, where the tail contains a much larger fraction of the bolometric luminosity. The disc emission in these spectra (variously termed very high or steep power law dominant state, hereafter VHS; Miyamoto et al. 1991; McClintock & Remillard 2003) is less obvious due to strong Comptonisation. Nonetheless, it can be identified in spectral fitting, but its derived parameters (temperature and luminosity) are somewhat dependent on how the tail is modelled. A simple power law description for the Comptonised tail can give a very misleading estimate of the accretion disc temperature. Where the seed photons for Comptonisation have a temperature which is close to (or within!) the observed bandpass then the shape of the Comptonised spectrum is *not* a power law. Instead there is a low energy break around the seed photon energy, decreasing the soft extent of the Comptonised component. This can significantly change the parameters of the inferred disc component (Done, Zycki & Smith 2002) and distort the measured luminosity-temperature relation (Kubota et al 2001; Kubota & Makishima 2004; KD04).

Using proper Comptonisation models for the tail approximately recovers a constant radius for the inner disc in the weakly Comptonised VHS spectra. The match is even better with an additional correction to the observed disc luminosity to account for the photons which are scattered into the Comptonised spectrum (Kubota et al 2001; Kubota & Makishima 2004; KD04). However, the most strongly Comptonised VHS (where the Comptonised component exceeds a half of the bolometric luminosity) have disk spectra which are not consistent with a constant disc radius even with such corrections (KD04). The simplest interpretation of these spectra is that the optically thick disc does not extend down to the last stable orbit in the strongly Comptonised VHS. This makes it geometrically rather similar to the low/hard state, where the hard emission is generally interpreted as arising from a hot inner flow replacing the inner optically thick disc (e.g. Narayan & Yi 1995). Such a geometry would also naturally explain the observed continuity of spectral properties as the spectra change from low/hard to VHS (e.g. Done & Gierlinski 2003). The timing properties also change in a smooth, correlated way from low/hard through strongly Comptonised VHS, with the low frequency QPO and power spectral break frequencies increasing (e.g. van der Klis 2004). This contrasts with the behaviour in the weak VHS, where the QPO frequency seems rather stable and has different characteristics (termed type B rather than type C), and with the lack of QPO's in the disc dominated spectra in the high/soft state. Therefore, both spectral and timing analyses are consistent with the idea that the disc structure is truncated at smaller radii going from the low/hard to strong VHS, while the disc extends down to the last stable orbit in the weak VHS and disc dominated high/soft states.

However, KD04 noted that an inner disc corona geometry for the optically thick Comptonising plasma meant that a larger inner radius was not the only explanation for the low disc temperature. The optically thick material could simply hide the inner disc from view and/or the power dissipated in the corona can *reduce* the disc emissivity (e.g. Svensson & Zdziarski 1994). We build explicit models of an inner disc-

corona to explore these ideas, and fit them to two broadband (simultaneous 0.7–200 keV ASCA and RXTE) spectra of Galactic black hole binary XTE J1550 – 564 to constrain the possible geometries of the disk-corona in the strongly Comptonized VHS.

In §2, we show the spectral parameters (luminosity and temperature) of the geometrically thin disk in the disk dominated high/soft state as a barometer to understand the disk parameters in the strongly Comptonized VHS. In §3 and §4, we describe the simultaneous ASCA-RXTE observations of the strongly Comptonized VHS and show that these imply a very different disc area and/or emissivity to that of the disc dominant state. In §5 we describe our model of an inner disc corona above a standard emissivity disc. Fitting this to the data shows explicitly that optical depth effects alone cannot hide the inner disc, and that this model requires a large change in disc area compared to the high/soft state. We modify this in §6 to incorporate energetic coupling of the inner disc and corona as in Svensson & Zdziarski (1994). The reduction in disc emissivity and temperature under the corona means this model can fit the observed spectra with only a small - or possibly no - increase in disc area. Additional spectral and timing characteristics of this state are discussed in §8, and they lead us to favour a coupled energetics disc-corona system in which the disc is additionally slightly truncated above the last stable orbit.

The robust result is that *all* the geometries considered here *require* that the inner disc changes in extent and/or emissivity: there are no solutions in which the inner disc has the same radial structure as that seen in the high/soft state. The disc structure *changes* in the presence of a strong corona.

2 THE DISK DOMINANT HIGH/SOFT STATE AS A BAROMETER OF GEOMETRY

We are primarily interested in *changes* in the disc emitting area rather than absolute values, in comparing the disc structure in the VHS with that seen in the disc dominated high/soft states. The high/soft states in XTE J1550 – 564 have been well fit using the DISKBB model (Mitsuda et al. 1984) in XSPEC (Kubota & Makishima 2004; Gierlinski & Done 2004; KD04), giving a clear $L \propto T_{in}^4$ relationship, implying constant area, over a factor 100 change in disc luminosity. Such an obviously thermal relationship between luminosity and temperature from DISKBB fits is now predicted by the best current models of the disc spectra which include radiative transfer with full metal opacities as well as relativistic effects (Davies et al 2005). Previous models which claimed a large change in colour temperature (which breaks the $L \propto T_{in}^4$ relationship) did not include metal opacities (Merloni et al 2000).

In all the following we use the binary system parameters determined by the optical studies of Orosz et al. (2002) i.e. mass of 8.4–11.2 M_{\odot} , distance, D , of ~ 5 kpc and binary inclination angle, i , of 70° (Orosz et al. 2002).

The apparent inner disc radius of this source, r_{in} , is obtained by from the normalization of DISKBB model, defined as $r_{in}^2 \cos i / (D/10\text{kpc})^2$. The average value inferred from all the high/soft state constant area DISKBB results is 59 km. However, the 'true' inner disc radius is related to this appar-

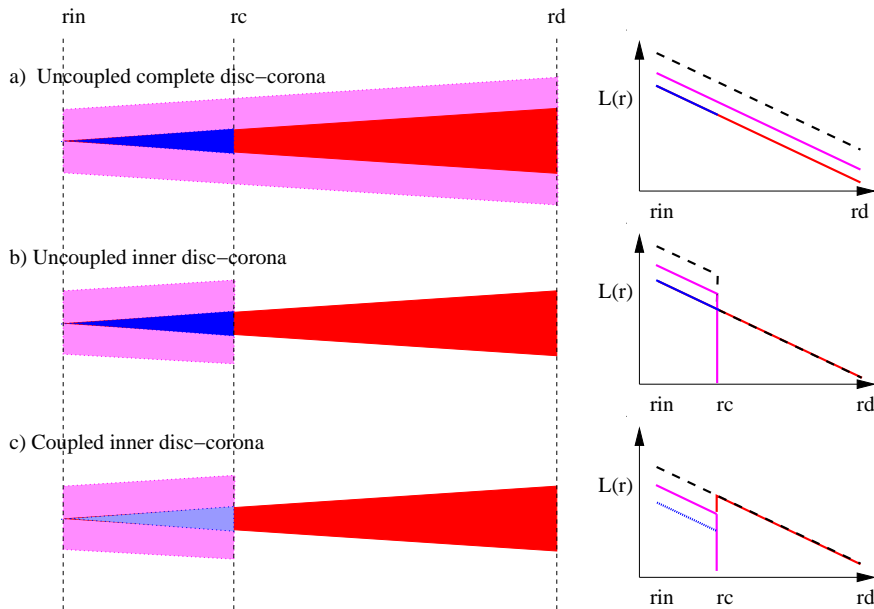


Figure 1. The schematic geometry envisaged for each of the models described in the text. To the right of each geometry is a sketch of the associated emissivity as a function of radius for the outer disc (red), inner disc (blue), corona (magenta) and total (black) accretion flow.

ent radius via a series of correction factors (for the stress free inner boundary condition, effective temperature not equal to colour temperature and relativistic effects; e.g. Kubota et al 1998; 2001). However, the fractional *change* in inferred disc radius is unaffected by uncertainties in distance, inclination and correction factors, so we give the apparent inner radius, r_{in} as a *ratio* of DISKBB normalisation seen in these fits to that derived from all the high/soft state data in Kubota & Makishima (2004).

3 ASCA-RXTE SIMULTANEOUS OBSERVATIONS

ASCA observations of this source were performed three times, on 1998 September 12, 23, and 1999 March 17. There are simultaneous *RXTE* observations corresponding to each ASCA observation. The second data set shows a strongly Comptonised VHS spectrum, and was included in the analysis of KD04. Here we also study the first simultaneous data set, which is at the boundary between the low/hard state and the strongly Comptonised VHS. We do not use the third ASCA dataset as the gain was changed on the corresponding *RXTE* data dataset midway through the observation, and the spectrum is only a weakly Comptonised VHS. The observational ID of the corresponding *RXTE* data are 30188-06-05-00 and 30191-01-10-00, for the first and second ASCA observations, respectively. Good PCA and HEXTE data were selected and processed, following standard procedures as described in KD04. The PCA response matrix was made for each observation by utilizing the latest version (8.0) of the software package *pcarsp*. This solves the well known calibration issues between *RXTE* and ASCA seen in previous *RXTE* responses (e.g. Done, Madejski & Zycki 2000).

The ASCA GIS events were extracted from circular re-

gions of $6'$ radius centered on the image peak, after selecting good time intervals in a standard procedure. Net exposures of 1.4 ks and 2.4 ks were obtained for the simultaneous pointing on the first and second observations, respectively. The dead time correction fractions for the first ASCA data set are 76.1% for GIS2 and 77.9% for GIS3, determined by reference to the count-rate monitor data with little dead time, using the method described in Makishima et al (1996). Similarly, for the second observaion, these are calculated as 85.6% and 87.3% for GIS2 and GIS3, respectively. We only use the GIS data since the SIS is strongly affected by pileup.

In order to take into account the calibration uncertainties, 0.5% systematic errors are added to each bin of the PCA and HEXTE spectra, and 1% systematic errors are for the GIS spectra. We use Morrison & McCammon (1983) abundances, and allow N_H to be free as the low energy bandpass of the ASCA GIS constrains this parameter. The data from different instruments are fitted with same model parameters except that relative normalization factors are free. Hereafter, we use the normalization of the PCA in the fitting results so as to be able to directly compare with the PCA analysis of Kubota & Makishima (2004). Using this we find the observed (i.e. absorbed) 0.7–200 keV fluxes of $7.2 \times 10^{-8} \text{ erg s}^{-1} \text{ cm}^{-2}$ and $8.3 \times 10^{-8} \text{ erg s}^{-1} \text{ cm}^{-2}$ on the 1st and 2nd simultaneous observations, respectively, corresponding to observed luminosities of $2.2 \times 10^{38} \text{ erg s}^{-1}$ and $2.5 \times 10^{38} \text{ erg s}^{-1}$ for isotropic emission. Correcting for absorption and the energy band gives a bolometric luminosity of ~ 4.0 and $4.7 \times 10^{38} \text{ erg s}^{-1}$ i.e. about 35 per cent of the Eddington limit.

4 CONTINUOUS DISC-CORONA

4.1 Previous spectral fits

These VHS spectra are dominated by the Compton scattered emission rather than the disc. The Comptonised emission has a complex spectral shape, showing features from both thermal and non-thermal electrons (e.g. Gierliński & Done 2003). Here we follow KD04 and approximate this by using the THCOMP model (Zdziarski, Johnson & Magdziarz 1996) to describe the thermal Compton scattering, together with a power law of Γ fixed at 2 to model the higher energy (non-thermal) emission. The seed photons in THCOMP are set to be from the disc (giving a slightly different low energy rollover to that produced by the COMPTT model in the XSPEC general release which assumes a Wien distribution). This is equivalent to assuming that the Comptonising corona covers the whole disc, as shown schematically in Fig. 1a.

Following KD04 we use several different descriptions of the reflected emission, to try to assess the effect on the derived disc parameters of systematic uncertainties in current reflection models. First we use the phenomenological gaussian plus smeared edge (SEG), and compare this with the results using the more physical reflection model incorporated in THCOMP. While this includes both continuum and self consistent iron line emission for arbitrary ionisation state of the reflected material (Zycki, Done & Smith 1999), it does not include Compton up and downscattering of the reflected emission in the disc itself. This can be very important for highly ionised and/or hot discs, and leads to strong distortions on the line and edge shapes (Ross, Fabian & Young 1999; Ballantyne, Ross & Fabian 2001). Thus we follow KD04 and remove the 5-12 keV region (covering the iron line and edge features which are sensitive to the disc Comptonisation) from the data, and refit the spectra with ionisation of the reflector fixed at 10^2 (Xi2), 10^3 (Xi3) and 10^4 (Xi4). Table 1 shows fitting results, and Fig. 2a and b shows each νF_ν spectrum, deconvolved and corrected for absorption using the best fit model (with phenomenological SEG reflection), together with residuals. The two spectra are qualitatively similar, with the disc emission being strongly Comptonised. The only differences are that the uncomptonised disc spectrum is slightly easier to identify in the first spectrum than in the second, and the spectral index of the Comptonised emission is slightly flatter. Both spectra show two clear breaks within the bandpass of the data, a high energy downturn at ~ 30 keV and a low energy downturn at 1.2 keV and 1.8 keV for the first and second data, respectively. We stress that the low energy downturns seen in these data are *not* due to absorption, since the spectra in these figures are absorption corrected, and this correction is fairly unambiguous. Absorption gives a characteristic, very sharp low energy cutoff in the GIS data, with a quite different shape than that inferred here for the intrinsic spectrum.

The existence of the low and high energy cutoffs within the observed 0.7–200 keV bandpass mean that these data cover the majority of the accretion power output. Thus the total luminosity is well defined, rather than being strongly affected by uncertainties associated with extrapolating the spectral models outside of the observed range.

4.2 Derived luminosity and temperature of the disc emission

Since the direct disc emission cannot easily be seen, then it initially appears that any reconstruction of the intrinsic disc spectrum, deconvolving the effects of the strong Comptonisation, must be fraught with uncertainty. However, this is *not* the case for broad bandpass spectra, where the energy range of the expected disc temperature is covered by the observations as in these ASCA-RXTE data. The reason is that the Comptonised spectrum itself contains a low energy rollover, directly imprinting the energy of the seed photons on the boosted emission.

The seed photon luminosity is equally observable, despite the effects of Comptonisation shrouding the disc, as the observed Comptonised emission *must* have originally come from the disc. Compton scattering increases the photon energy by on average $\Delta E/E \sim 4\tau^2(kT_e/m_e c^2)$. Thus the Comptonised luminosity is related to the scattered disc luminosity simply by a factor $\sim (1 + \Delta E/E) \sim 1.3$ for the steep Comptonised spectra observed here. This scattered disc luminosity should simply be added to the observed disc luminosity to estimate the intrinsic disc luminosity of $L_{disc} + L_{thcomp}/1.3 \approx L_{disc} + L_{thcomp}$. Thus the intrinsic disc luminosity cannot be very much smaller than the total luminosity, which is robustly estimated by these data. This is shown plotted against observed disc temperature in Fig ??a, and plainly shows a marked discrepancy with the constant radius/constant colour temperature correction observed from the disc dominated spectra.

A more careful correction for the effects of Compton scattering can be done by noting that this conserves photon number so the intrinsic disc luminosity can be simply estimated by increasing the *observed* disc luminosity by a factor $(aN_{comp} + N_{disc})/N_{disc}$ where N_{comp} and N_{disc} are the numbers of photons in the thermally Comptonised and disc spectral components, respectively, and a are $2\cos i$ and 1 for spherical and slab geometries (see Kubota & Makishima 2004; KD04). Panel b shows the reconstructed disc luminosity assuming a slab geometry and clearly shows that the inferred disc is very different to that seen in the high/soft state data.

Thus, while spectral fitting is almost always non-unique, the presence of the low and high energy rollover in the observed bandpass mean that we can make very robust estimates for the *intrinsic* disc temperature and luminosity, giving a marked discrepancy with the constant radius/constant colour temperature correction observed from the disc dominated spectra. Disc dominated spectra at the same luminosity have a temperature of ~ 1 keV, so for a spectrum dominated by Comptonisation we expect a low energy rollover from the seed photon energy at $4kT_{in} \sim 4$ keV. This is in direct conflict with the observation of the low energy rollover at 1.2 keV or 1.8 keV which shows the seed photon temperature is < 0.5 keV or < 0.7 keV. The inferred disc is highly luminous but with low temperature, implying that the inner radius of the disc is a factor ~ 3 higher in the VHS than in the disc dominated spectra.

Plainly, with these models the disc is *not* consistent with a constant inner radius, constant emissivity, constant colour temperature correction between the VHS and the disc dominated state. At least one of these *must* be changing. An

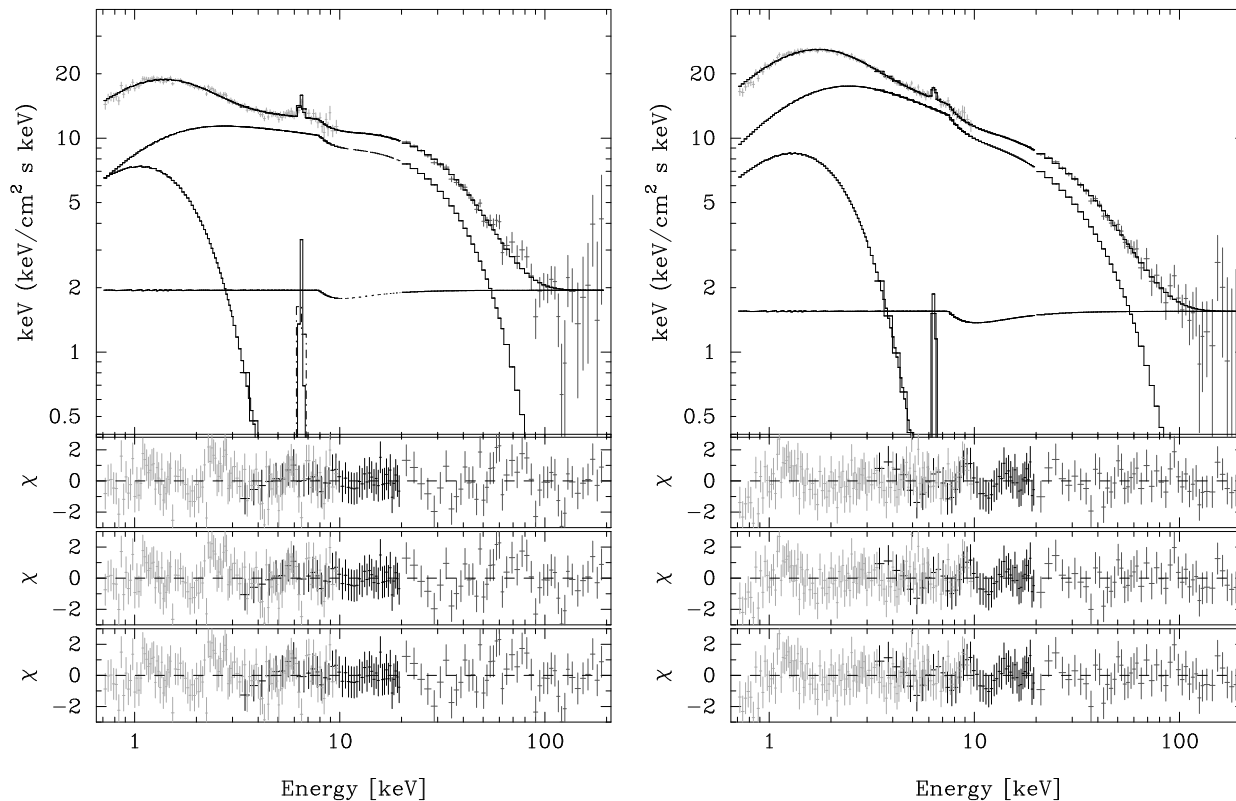


Figure 2. Absorption corrected intrinsic spectra for each of the two observations described in the text. The left and right hand panels show the simultaneous ASCA-RXTE data taken before and after the peak, respectively. Both datasets are deconvolved using the best fit phenomenological model with SEG reflection, and the ASCA and HEXTE normalisations are set to match the PCA. The residuals are from this fit (SEG in Table 1), the DKBBTH fits (SEG in Table 2) and the DKBBFTH fits (SEG in Table 3), respectively, showing that all these different disc-corona models are a good description of the overall spectral shape.

obvious change is for the corona to affect the colour temperature correction. Irradiation will change the vertical temperature structure of the disc, but this should lead to an *increasing* temperature for the upper layers, so an *increased* colour temperature correction. Yet the data show a *lower* temperature for the inferred luminosity. Similarly, conduction between the corona and disc would also increase the disc temperature, as would an increase in the stress at the inner disc boundary (Agol & Krolik 2000). This robust discrepancy between the disc structure in the disc dominated and VHS motivates the more sophisticated modelling in the rest of the paper.

5 INNER DISC CORONA, SEPARATE ENERGETICS

5.1 Models

Here we build a simple model of an inner disc corona, incorporating the effects of the geometry as well as the radiative constraints from Comptonisation. The corona only exists at small radii, so it removes the hot inner disc spectrum by Comptonising it, while not affecting the spectrum of the cooler disc at larger radii. The aim is to test whether this more physically realistic model still requires the inferred increase in disc inner radius seen in the previous section.

We assume that the corona is a slab of constant optical depth and temperature on top of the disc, extending from r_{in} to r_c , while the disc itself extends from r_{in} to $1000r_{\text{in}}$ (see Fig. 1b). Each radius in the disc is assumed to emit blackbody radiation, with the standard temperature distribution of a multicolour DISKBB i.e. $T(r) = T_{\text{in}}(r/r_{\text{in}})^{-3/4}$. Where the disc is not covered by the Compton slab then its emission is unaffected. Otherwise, it is suppressed by a factor $\exp(-\tau)$, where τ is determined from the Comptonised spectrum using the observed Γ and kT_e , assuming a slab geometry. The blackbody emission from the disc at this radius is used as the seed photons for the Comptonising cloud, whose spectrum is then normalised so that the total number of photons in the Comptonised spectrum is equal to the number of photons scattered from the blackbody disc emission at that radius i.e. $1 - \exp(-\tau)$.

A more careful treatment would have to account for the different angle dependences of the seed photons and comptonised emission - the number of seed photons which emerge unscattered is more accurately $\exp(-\tau/\cos i)$, but the number which are scattered into this direction is *not* simply $1 - \exp(-\tau/\cos i)$ as photons scattered into a given line of sight come from a range of initial seed photon angles (see e.g. Pozdnyakov, Sobol & Sunyaev 1983). There is yet more complexity as about half the compton scattered photons will be directed down towards the disc. Those which

Table 1. Best fit parameters obtained by a simultaneous *ASCA/RXTE* observation. The continuum is always described by a multi-colour disc spectrum, plus a low temperature thermal comptonised component, together with a power law extending to high energies. The five different fits show the results of the different descriptions of reflection. These are a narrow gaussian line and smeared edge in SEG, while the other models include the full reflection spectrum (line and continuum) in the *thcomp* model. In the case of Xi1, Xi2 and Xi3, the data in 5–12 keV is excluded from the spectral fit, R_{in} is fixed to 30 R_{g} , and the value of ξ is fixed to 10^2 , 10^3 , 10^4 , for models Xi1, Xi2, and Xi3, respectively. Normalization factors with the PCA data are used to calculate luminosities.

model	N_{H} 10^{21}cm^{-2}	T_{in} keV	Γ_{thc}	T_{e} keV	L_{disk} (N_{disk})	$L_{\text{thc(slab)}}$ (N_{thc})	L_{pow}	smedge,line (a) reflection (b–e)	χ^2/dof
Before peak									
SEG	6.5 ± 0.2	$0.45^{+0.02}_{-0.01}$	$2.08^{+0.01}_{-0.02}$	10.0 ± 0.5	1.03 (37.6)	3.14 (58.0)	0.86	$E = 7.9^{+0.3}_{-0.2}$ keV $\tau_{\text{max}} = 0.3^{+0.2}_{-0.1}$ width= 3^{+2}_{-1} keV $E = 6.48^{+0.03}_{-0.07}$ keV EW=81 ± 10 eV	201.4/192
REF	5.9 ± 0.1	$0.51^{+0.01}_{-0.02}$	2.10 ± 0.01	$11.6^{+0.5}_{-0.6}$	0.92 (30.1)	3.05/2.64 (51.0/44.9)	0.76	$\Omega/2\pi = 0.23^{+0.04}_{-0.01}$ $\xi = 6.8^{+0.8}_{-2.7} \times 10^3$ $R_{\text{in}} = 94^{+159}_{-83} R_{\text{g}}$	230.2/194
Xi1	$6.5^{+0.2}_{-0.3}$	0.45 ± 0.03	$2.27^{+0.02}_{-0.03}$	14 ± 1	0.86 (31.0)	3.52/2.95 (80.2/64.4)	0.76	$\Omega/2\pi = 0.76^{+0.08}_{-0.06}$ ($\xi = 10^2$)	146.3/146
Xi2	$6.1^{+0.02}_{-0.01}$	0.50 ± 0.02	2.14 ± 0.01	11.5 ± 6	0.90 (29.8)	3.14/2.69 (57.0/48.5)	0.81	$\Omega/2\pi = 0.37 \pm 0.07$ ($\xi = 10^3$)	161.2/146
Xi3	6.2 ± 0.2	0.48 ± 0.02	2.10 ± 0.01	11.3 ± 0.6	0.97 (33.5)	3.10/2.41 (53.5/42.7)	0.81	$\Omega/2\pi = 0.42^{+0.08}_{-0.04}$ ($\xi = 10^4$)	157.8/146
After peak									
SEG	6.7 ± 0.2	0.55 ± 0.02	$2.32^{+0.02}_{-0.03}$	12 ± 1	1.19 (36.1)	4.09 (80.9)	0.69	$E = 7.5 \pm 0.2$ keV $\tau_{\text{max}} = 0.6 \pm 0.2$ width= 5^{+3}_{-2} keV $E = 6.4 \pm 0.1$ keV EW=41 $^{+12}_{-6}$ eV	157.8/192
REF	7.1 ± 0.1	$0.44^{+0.06}_{-0.02}$	2.74 ± 0.03	$> 120^{\text{a}}$	0 (0)	5.87/5.32 (163.9/161.9)	0.29	$\Omega/2\pi = 1.7^{+0.2}_{-0.1}$ $\xi = 5^{+2}_{-1}$ $R_{\text{in}} = 12 \pm 2 R_{\text{g}}$	226.2/194
Xi1	$7.1^{+0.3}_{-0.2}$	0.53 ± 0.03	2.64 ± 0.03	38^{+18}_{-9}	0.89 (27.6)	5.20/4.00 (139.5/98.5)	0.46	$\Omega/2\pi = 1.6^{+0.3}_{-0.2}$ ($\xi = 10^2$)	113.5/146
Xi2	6.5 ± 0.3	0.60 ± 0.02	2.42 ± 0.02	16 ± 2	1.17 (32.9)	4.10/3.29 (80.9/64.4)	0.62	$\Omega/2\pi = 0.73^{+0.05}_{-0.09}$ ($\xi = 10^3$)	131.6/146
Xi3	$6.6^{+0.03}_{-0.01}$	$0.55^{+0.02}_{-0.03}$	$2.35^{+0.02}_{-0.01}$	14^{+2}_{-1}	1.13 (34.2)	4.18/3.16 (80.8/63.1)	0.64	$\Omega/2\pi = 0.62^{+0.04}_{-0.08}$ ($\xi = 10^4$)	127.9/146

^a The best fit value appeared in > 200 keV.

are not reflected will be reprocessed, adding to the intrinsic disc emission (Haardt & Maraschi 1993). We neglect all these effects in order to be able to approximately calculate the spectrum.

The shape of the spectrum is determined by the parameters of the Compton corona (Γ and kT_{e}), the size of this corona relative to the disc $r_{\text{c}}/r_{\text{in}}$, and intrinsic inner disc temperature, kT_{in} . The overall normalisation gives the apparent disc radius, r_{in} , for the assumed distance and inclination, as in the DISKBB model. Even though the full DISKBB spectrum *is not* seen, the model normalisation is that of the

uncomptonised disk. The model parameters for the disk component are in effect what the disk would have looked like without the comptonising corona, and so can be directly compared with the disk normalisation derived from the disk dominant high/soft state.

Fig. 4a shows the results for this model corona parameters close to those implied by the VHS data i.e. a corona with $kT_{\text{e}} = 10$ keV and $\tau = 2$ (which corresponds to a photon index of the scattered flux of $\Gamma = 2.3$ as the optical depth for a slab geometry is half of that which gives the same spectrum for a sphere). The inner disc temperature is set to 1 keV to

Table 2. Same as Table 1 but with DKBBTH instead of DISKBB plus THCOMP to describe a simple (uncoupled energetics) inner disc-corona.

model	N_{H} 10^{21}cm^{-1}	T_{in} keV	r_{in} [km]	R_c/r_{in}	Γ_{thc}	T_e keV	disk-corona ^a	smedge reflection	χ^2/dof
Before peak									
SEG	$6.6^{+0.2}_{-0.3}$	$0.60^{+0.04}_{-0.02}$	129^{+10}_{-18}	$1.59^{+0.03}_{-0.02}$	$2.08^{+0.01}_{-0.02}$	$9.9^{+0.4}_{-0.6}$	$L = 4.20$ $L_{\text{disc}}^{\text{int}} = 2.79$ $\tau = 2.3$	$E = 8.0^{+0.2}_{-0.1}$ $\tau_{\text{max}} = 0.29^{+0.26}_{-0.08}$ width = $2.6^{+0.2}_{-1.6}$ $E = 6.48 \pm 0.07$ EW = 80 ± 10 [eV]	204.9/192
REF	6.1 ± 0.2	0.64 ± 0.02	107^{+5}_{-6}	$1.58^{+0.01}_{-0.02}$	2.11 ± 0.02	11.8 ± 0.4	$L = 4.04$ $L_{\text{disc}}^{\text{int}} = 2.48$ $\tau = 2.0$	$\Omega/2\pi = 0.32^{+0.02}_{-0.05}$ $\xi = (3.4^{+1.5}_{-1.2}) \times 10^3$ $R_{\text{in}} = 180^{+410}_{-100}$	227.3/194
Xi1	6.7 ± 0.2	$0.57^{+0.06}_{-0.04}$	170^{+20}_{-50}	$1.72^{+0.05}_{-0.04}$	2.27 ± 0.03	14 ± 1	$L = 4.32$ $L_{\text{disc}}^{\text{int}} = 3.81$ $\tau = 1.6$	$\Omega/2\pi = 1.0 \pm 0.2$	148.9/146
Xi2	$6.2^{+0.3}_{-0.1}$	$0.63^{+0.05}_{-0.02}$	110^{+20}_{-15}	1.57 ± 0.03	2.12 ± 0.01	$11.4^{+0.5}_{-0.4}$	$L = 4.04$ $L_{\text{disc}}^{\text{int}} = 2.46$ $\tau = 2.0$	$\Omega/2\pi = 0.48^{+0.10}_{-0.08}$	159.6/146
Xi3	$6.1^{+0.2}_{-0.4}$	$0.62^{+0.02}_{-0.04}$	110^{+20}_{-7}	1.46 ± 0.03	$2.094^{+0.007}_{-0.008}$	$11.3^{+0.6}_{-0.5}$	$L = 3.98$ $L_{\text{disc}}^{\text{int}} = 2.31$ $\tau = 2.1$	$\Omega/2\pi = 0.7 \pm 0.1$	157.0/146
After peak									
SEG	6.9 ± 0.2	0.71 ± 0.03	110^{+6}_{-12}	1.70 ± 0.05	$2.32^{+0.02}_{-0.03}$	12 ± 1	$L = 5.37$ $L_{\text{disc}}^{\text{int}} = 3.97$ $\tau = 1.7$	$E = 7.6 \pm 0.2$ $\tau_{\text{max}} = 0.5^{+0.3}_{-0.2}$ width = 4^{+3}_{-2} $E = 6.39 \pm 0.08$ EW = 50 ± 10 [eV]	151.1/192
REF	6.6 ± 0.1	$0.72^{+0.02}_{-0.05}$	105^{+11}_{-9}	$1.9^{+0.2}_{-0.1}$	$2.46^{+0.08}_{-0.03}$	20 ± 1	$L = 5.33$ $L_{\text{disc}}^{\text{int}} = 3.83$ $\tau = 1.1$	$\Omega/2\pi = 0.64^{+0.13}_{-0.04}$ $\xi = (1.4^{+0.3}_{-0.5}) \times 10^2$ $R_{\text{in}} = 31^{+8}_{-9}$	228.5/194
Xi1	6.9 ± 0.1	$0.64^{+0.04}_{-0.03}$	130 ± 15	$2.2^{+0.3}_{-0.2}$	$2.58^{+0.02}_{-0.03}$	20^{+2}_{-1}	$L = 5.48$ $L_{\text{disc}}^{\text{int}} = 3.66$ $\tau = 1.0$	$\Omega/2\pi = 1.2^{+0.2}_{-0.4}$	127.0/146
Xi12	$6.8^{+0.2}_{-0.3}$	$0.70^{+0.03}_{-0.05}$	110^{+17}_{-10}	1.7 ± 0.1	$2.40^{+0.02}_{-0.01}$	16^{+2}_{-1}	$L = 5.35$ $L_{\text{disc}}^{\text{int}} = 3.75$ $\tau = 1.4$	$\Omega/2\pi = 0.6 \pm 0.1$	121.2/146
Xi13	6.8 ± 0.2	0.66 ± 0.03	120 ± 10	$1.52^{+0.03}_{-0.05}$	$2.355^{0.008}_{-0.012}$	16 ± 1	$L = 5.37$ $L_{\text{disc}}^{\text{int}} = 3.47$ $\tau = 1.4$	$\Omega/2\pi = 0.9^{+0.2}_{-0.1}$	124.2/146

^a The unabsorbed bolometric luminosity of the DKBBTH, L , is calculated for inclination 70° by integrating the model spectrum by 0.001–300 keV. The intrinsic disc luminosity, $L_{\text{disc}}^{\text{int}}$, is calculated by referring to observed r_{in} and T_{in} as $4\pi r_{\text{in}}^2 \sigma T_{\text{in}}^4$.

match that seen from the disc dominated spectra at similar luminosities (see Fig. ??). The radius of the Comptonising region is progressively increased over more and more of the disc, from $r_c/r_{\text{in}} = 1, 1.33, 1.66, 3.33$ and 1000. This changes the spectrum from a pure disc blackbody, to a more complex shape. While this does have the same number of free parameters as the previous model, it is somewhat more constrained. The normalisation of the disc and Comptonised components is not a completely free parameter, but is set by r_c/r_{in} and by the assumed slab geometry. In the limit

where the corona covers all the disc then the spectrum has the same shape as that of a THCOMP model with disc blackbody seed photons but with the addition of $\exp(-\tau)$ of the initial disc blackbody spectrum which is unscattered by the corona.

The spectrum *always* shows the imprint of the seed photon energy at ~ 1 keV. This is because of the physical requirements of the model, firstly that the seed photons are from the inner disc with standard emissivity, and secondly that the Comptonised spectrum has the same number of

Table 3. Same as Table 1 but with DKBBFTH instead of DISKBB plus THCOMP to describe an inner disc-corona with coupled energetics.

model	N_{H} 10^{21}cm^{-1}	$T_{\text{in}}^{\text{int}}$ keV	r_{in} [km]	$R_{\text{c}}/r_{\text{in}}$	Γ_{thc} keV	T_{e}	disc-corona ^a	smedge reflection	χ^2/dof
Before peak									
SEG	6.4 ± 0.1	$0.88_{-0.04}^{+0.03}$	71_{-5}^{+10}	$2.46_{-0.09}^{+0.05}$	2.07 ± 0.02	9.8 ± 0.5	$L = 4.03(3.90)$ $f = 0.58$ $\tau = 2.3$	$E = 8.0_{-0.3}^{+0.2}$ $\tau_{\text{max}} = 0.3_{-0.1}^{+0.3}$ width = 3_{-1}^{+3} $E = 6.48 \pm 0.07$ EW = 85 ± 10	204.7/192
REF	6.1 ± 0.1	0.91 ± 0.02	65_{-1}^{+3}	$2.3_{-0.05}^{+0.07}$	$2.111_{-0.005}^{+0.007}$	$11.6_{-0.4}^{+0.8}$	$L = 3.94(3.73)$ $f = 0.56$ $\tau = 2.0$	$\Omega/2\pi = 0.31_{-0.2}^{+0.04}$ $\xi = (2.7_{-0.5}^{+2.0}) \times 10^3$ $R_{\text{in}} = 160_{-80}^{+900}$	230.9/194
Xi1	6.4 ± 0.1	$0.80_{-0.04}^{+0.06}$	84_{-13}^{+11}	$2.43_{-0.07}^{+0.06}$	$2.26_{-0.03}^{+0.02}$	$13.7_{-1.1}^{+0.5}$	$L = 3.73(3.73)$ $f = 0.51$ $\tau = 1.7$	$\Omega/2\pi = 0.9 \pm 0.02$	150.3/146
Xi2	6.1 ± 0.1	$0.89_{-0.05}^{+0.02}$	67_{-3}^{+8}	$2.3_{-0.1}^{+0.2}$	$2.137_{-0.009}^{+0.007}$	$11.5_{-0.8}^{+0.4}$	$L = 3.64(3.64)$ $f = 0.55$ $\tau = 2.0$	$\Omega/2\pi = 0.49_{-0.10}^{+0.09}$	159.3/146
Xi3	6.1 ± 0.1	$0.83_{-0.03}^{+0.04}$	75_{-6}^{+2}	$2.11_{-0.10}^{+0.06}$	$2.101_{-0.014}^{+0.002}$	$11.6_{-0.8}^{+0.2}$	$L = 3.43(3.45)$ $f = 0.56$ $\tau = 2.1$	$\Omega/2\pi = 0.70_{-0.14}^{+0.16}$	157.9/146
After peak									
SEG	6.7 ± 0.2	$0.95_{-0.02}^{+0.03}$	71_{-5}^{+7}	$2.32_{-0.07}^{+0.06}$	2.31 ± 0.02	12 ± 1	$L = 5.23(5.31)$ $f = 0.47$ $\tau = 1.7$	$E = 7.6 \pm 0.2$ $\tau_{\text{max}} = 0.5_{-0.2}^{+0.3}$ width = 4_{-2}^{+1} $E = 6.39 \pm 0.08$ EW = 50 ± 10	154.8/192
REF	$6.8_{-0.1}^{+0.3}$	$0.86_{-0.09}^{+0.02}$	86_{-7}^{+11}	$2.76_{-0.2}^{+0.3}$	$2.48_{-0.02}^{+0.03}$	$21.8_{-1.7}^{+0.5}$	$L = 5.48(5.23)$ $f = 0.39$ $\tau = 1.1$	$\Omega/2\pi = 0.7 \pm 0.1$ $\xi = (1.1 \pm 0.2) \times 10^2$ $R_{\text{in}} = 26_{-44}^{+9}$	207.2/194
Xi1	$7.2_{-0.1}^{+0.2}$	$0.74_{-0.04}^{+0.03}$	120 ± 20	2.9 ± 0.3	$2.57_{-0.05}^{+0.03}$	22_{-2}^{+1}	$L = 5.30(5.58)$ $f = 0.36$ $\tau = 0.97$	$\Omega/2\pi = 1.1_{-0.2}^{+0.1}$	114.8/146
Xi2	$6.7_{-0.01}^{+0.02}$	$0.89_{-0.04}^{+0.03}$	78_{-6}^{+2}	$2.20_{-0.09}^{+0.04}$	2.41 ± 0.01	16 ± 1	$L = 4.93(4.93)$ $f = 0.43$ $\tau = 1.4$	$\Omega/2\pi = 0.62_{-0.08}^{+0.10}$	123.2/146
Xi3	$6.7_{-0.01}^{+0.02}$	0.83 ± 0.03	85_{-6}^{+4}	$1.97_{-0.10}^{+0.06}$	$2.36_{-0.01}^{+0.03}$	17 ± 1	$L = 4.39(4.43)$ $f = 0.45$ $\tau = 1.4$	$\Omega/2\pi = 0.9_{-0.1}^{+0.3}$	128.1/146

^a The unabsorbed bolometric luminosity of the DKBBFTH, L , is calculated for inclination 70° by integrating the model spectrum by 0.001–300 keV. In this fit, the intrinsic disc luminosity calculated as $4\pi r_{\text{in}}^2 \sigma T_{\text{in}}^{\text{int}4}$ is naturally the same as the bolometric luminosity, L , by definition, and it is shown in parenthesis. The slight difference comes from ***

photons in it as were removed from the disc emission. A standard disc emissivity disc produces most of its luminosity in the inner regions, and it is these inner regions which are covered by the corona. The Compton energy boost is not large for these coronal parameters ($\Gamma = 2.3$, $kT_{\text{e}} = 10$ keV) so the Comptonised photons, with their clear seed photon rollover, add to the emission at similar energies to those of the seed photons. Comptonisation conserves photon number, so the normalisation of the spectrum is also similar.

Thus the optically thick corona does intercept most of the inner disc emission, but this Comptonisation does not hide it as neither the energy nor number of photons are changed substantially.

Figure 4b shows the same series of spectra for increasing coronal radius, but with $kT_{\text{e}} = 100$ keV. Though increasing the electron temperature increases the energy boost so making it possible to move the photons away from their seed energy, to get the same spectral index of $\Gamma = 2.3$ from this

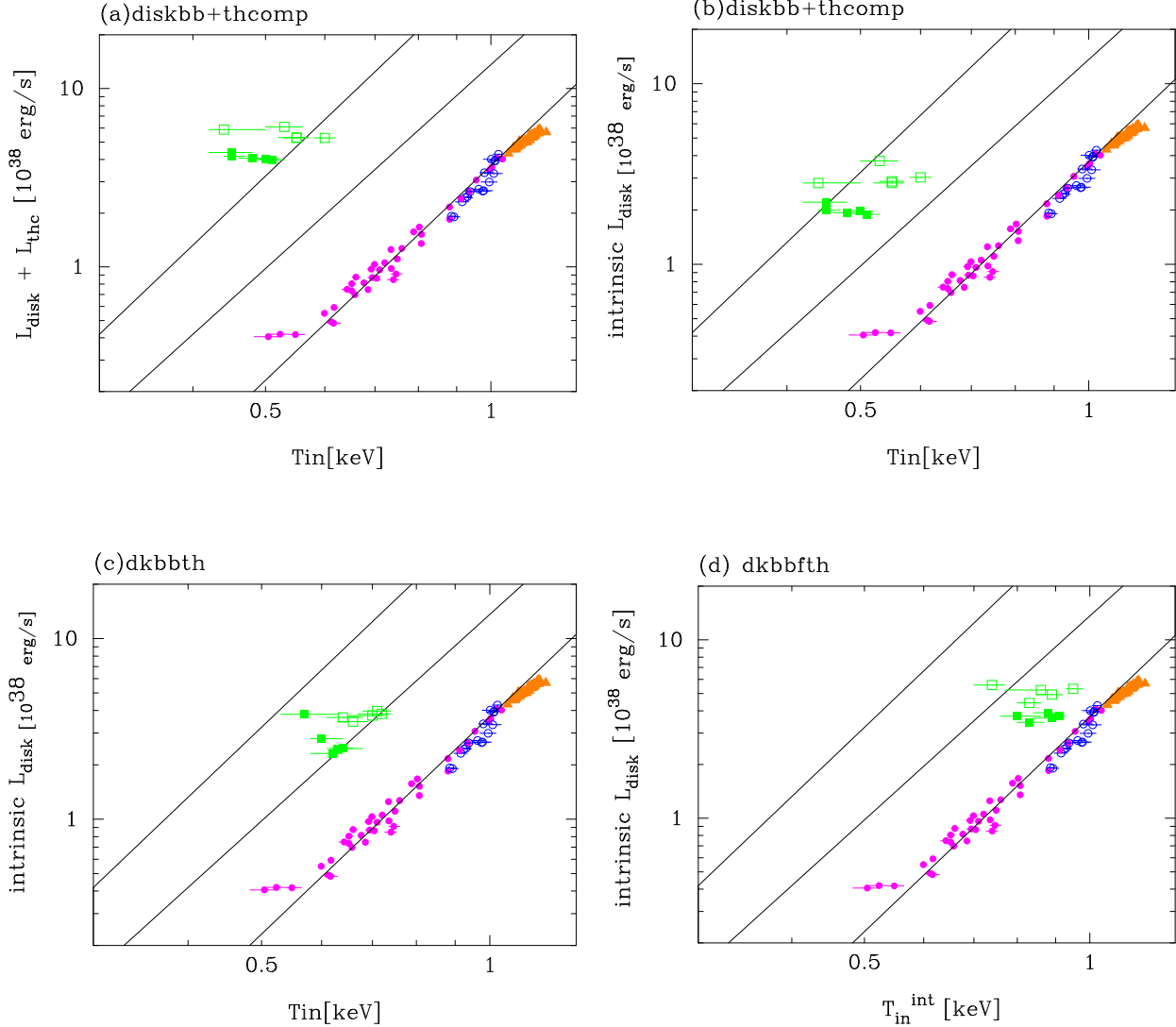


Figure 3. Luminosity versus temperature plots for the disc. Filled circles and filled triangles show the data from the disc dominated states, while the open circles show the weakly comptonised very high state (KD04). Filled and open squares and open squares show the strongly comptonised very high state data from before and after the peak, respectively. There are five points for each of these strongly comptonised spectra, corresponding to the five different reflection descriptions. The solid lines show $L \propto T^4$ for $r_{\text{in}} = 59, 100$ and 200 km. Panel a and b show the reconstructed disc emission from simple modelling of the spectra (Table 1), corresponding to a corona covering the whole disc (see Fig. 1a). Panel a plots the observed disc temperature against the inferred disc luminosity estimated by $L_{\text{disc}} + L_{\text{thcomp}}$. This is a slight overestimate since comptonisation boosts the seed photon luminosity by a factor ~ 1.3 for these data. Panel b shows a more careful reconstruction of the disc luminosity using the photon numbers and inclination of the slab. Either way gives similar results, showing that the inferred disc luminosity and temperature is quite robustly estimated by these data, and that they imply the inner edge of the disc is much larger than that seen in the disc dominated spectra. Panel c shows the reconstructed inner disc temperature and luminosity for an inner disc-corona (Fig. 1b). This is not very different to that found from the previous fits. By contrast, Panel d shows the results for an inner disc whose energetics are coupled to that of the corona (Fig. 1c). The implied change in inner disc radius is now much smaller.

higher temperature plasma requires a lower optical depth. The corona becomes optically thin so the spectrum now is clearly always two component (disc plus Comptonisation), and the disc is always also clearly at 1 keV. Although only the inner disc photons are now boosted far away from their seed photon energy, the low optical depth means that not enough of them are Comptonised to hide the hottest disc components even for a corona that extends over the whole disc.

A comparison by eye of these models with the observed spectra in Fig. 2 shows that the observed low energy rollover at ~ 1.8 keV strongly constrains the seed photon energy even in an inner disc corona model to be substantially less than 1 keV. Thus this model is *not* going to easily change the conclusion of the previous section that the inner disc temperature is much lower than is seen at this luminosity in the disc dominated high/soft states. These models of an inner disc corona above a standard emissivity disc still re-

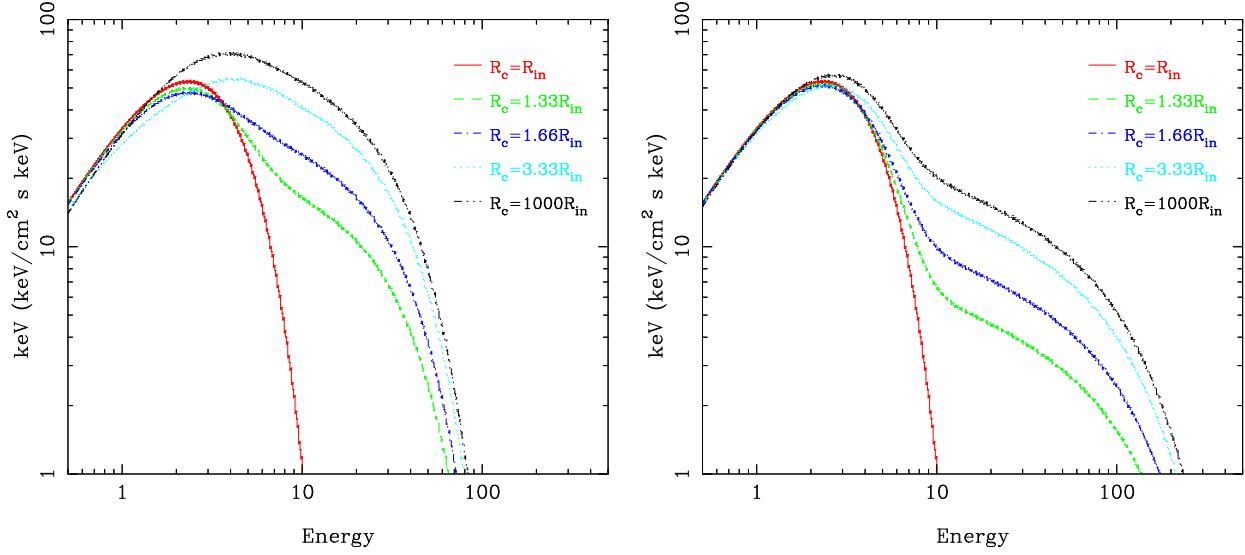


Figure 4. An inner disc corona model for $r_c = 1$ (red, i.e. equivalent to no corona), 1.33 (green), 1.66 (blue), 3.33 (cyan) and 1000 (black i.e. equivalent to a corona which completely covers the disc) $\times r_{in}$ (see Fig. 1b). The left panel shows the results for coronal parameters close to those inferred from the data, with $\Gamma = 2.3$ and $kT_e = 10$ keV. This corresponds to $\tau \sim 2$ for a slab corona. The right panel shows the effect of increasing the coronal temperature to 100 keV. To keep the same spectral index for higher temperature means that the optical depth has to decrease to $\tau \sim 0.4$. Thus there is always a clear unscattered disc component (unlike the data), and the intrinsic disc temperature of 1 keV is seen.

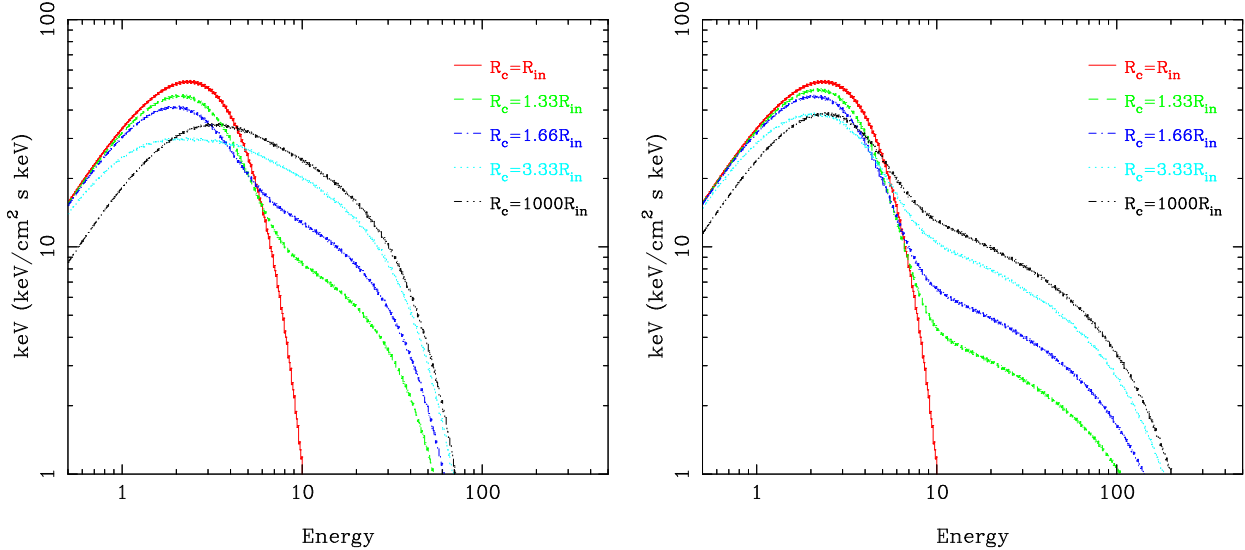


Figure 5. As in Fig.4, but for an inner disc-corona with coupled energetics (see Fig. 1c). The spectra left hand panel ($\Gamma = 2.3$, $kT_e = 10$ keV) have $f \sim 0.5$ for $r < r_c$, while those in the right hand panel ($\Gamma = 2.3$, $kT_e = 100$ keV) have $f \sim 0.3$.

quire that the disc inner radius in the VHS is substantially larger than in the high/soft disc dominated states.

5.2 Data fitting

We quantify the argument above by replacing the separate DISKBB and THCOMP components in the spectral fits with this new inner disc corona model. We include the THCOMP reflection model in the disc-corona code, to take into account illumination of the outer disc by the Comptonised spectrum.

Again we use the same range of ionized reflection descriptions as before in order to quantify the uncertainties which arise from our modeling of this component.

First we fit this model to the simultaneous ASCA-RXTE spectra with the coronal radius fixed at $r_c/r_{in} = 1000$. This model has one less free parameter than the separate DISKBB+THCOMP fits shown in § 4 because of the specific geometry (slab corona) assumed. The observed spectral shape of the Comptonised emission (Γ and kT_e) set τ for the specific geometry, and this fixes the ratio of nor-

malisations of disc and Comptonised emission. The fits are significantly worse, showing that our assumed specific continuous slab corona geometry is not consistent with the data. However, the inferred disc temperatures for the underlying standard emissivity DISKBB spectrum are ~ 0.48 keV and 0.51 keV for the first and second data set, respectively. These are much the same temperatures as for the previous fits (though with worse χ^2 due to the assumed geometry), illustrating the robustness of reconstruction of the seed photon (intrinsic disc) temperature

We then repeat the fits with the coronal radius as a free parameter to correspond to the geometry of Fig.1b (again with all five different reflection descriptions). While this formally gives the same number of degrees of freedom as the separate DISKBB+THCOMP fits, the model is more constrained by the geometric and physical assumptions. Nonetheless, the fits are indistinguishable in χ^2 from those in § 4, strongly supporting an inner disc-corona geometry for these VHS spectra. Table 2 gives the results for the underlying (i.e. intrinsic, before Comptonisation) DISKBB temperature and luminosity. These are plotted in the middle panel of Fig. ??b, together with the points from the disc dominated spectra (KD04). Plainly, as shown above, the ASCA-RXTE spectra still strongly require a very low temperature disc which does not fall on the constant radius/constant colour temperature correction line derived for the disc dominated spectra. Again the inferred apparent inner disc radius of $r_{\text{in}} \sim 110\text{--}130$ km is a factor 2 larger than the ~ 60 km seen in the high/soft disc dominated states.

6 INNER DISC CORONA, COUPLED ENERGETICS

6.1 Models

The previous model assumed that the disc emission is unaffected by the presence of the corona. That is, the inner disc corona model assumes that while the disc radiates efficiently at all radii, the coronal mass flow only radiates within r_c . However, this seems rather artificial. The corona dissipates some power, and this must derive ultimately from the accretion flow. The disc and coronal flows could be kept separate in a continuous corona geometry (e.g. Fig. 1a) with some (approximately constant) fraction of the power and/or mass accretion taking place via the corona (Zycki et al 1997, Haardt & Maraschi 1993; Svensson & Zdziarski 1994). The geometry of an inner disc-corona instead implies that there is a *single* accretion flow at large radii, $\dot{M}_{\text{disc},\infty}$ which then splits at r_c to form the disc and corona. Svensson & Zdziarski (1994) calculate the effect on the disc in the limit in which most of the mass accretion rate is still carried by the disc, but where a fraction f of the accretion power is dissipated in the corona. The power dissipated in the optically thick disc is discontinuous at r_c , where it drops from $\dot{M}_{\text{disc},\infty}$ by a factor $(1-f)$. This implies the disc temperature is also discontinuous, dropping to $(1-f)^{1/4}$ of that expected from $\dot{M}_{\text{disc},\infty}$. This is shown schematically in Fig. 1c.

We incorporate these ideas into our inner disc-corona code to predict the spectrum from a coupled disc-corona system. The code starts with the standard emissivity disk to produce an initial guess at the seed photon luminosity and

temperature and calculates the Comptonised flux as before (using Γ and kT_e to determine τ , and scattering a fraction $1 - \exp(-\tau)$ of the disc photons into the Comptonised emission). The total Comptonised flux from all radii is used to calculate a (radially averaged) value of f which is used to recalculate the disk emissivity and temperature, acting as seed photons for the Comptonising corona, giving a slightly different value of f . The code iterates once more around this loop in order to reach a self-consistent solution. The parameters of the model are the same as for the uncoupled inner disc-corona system described above. Again, the inner disc temperature is that of the *uncomptonised* disk i.e. the DISKBB which would have been seen *without* the corona present. For the uncoupled disk-corona this is simply the underlying disc emission, whereas for the coupled disk-corona the underlying disc emission is distorted from that of a DISKBB by the effect of the corona draining energy from the disk. The 'temperature' which parameterises this coupled disk-corona systems is the innermost disc temperature, $T_{\text{in}}^{\text{int}}$, which would be seen in the limit of $f = 0$, *not* the inner disc temperature used in making the model which is $(1-f)^{1/4}T_{\text{in}}^{\text{int}}$.

Fig. 5a and b shows the spectra obtained from such models with the same intrinsic disc ($T_{\text{in}}^{\text{int}} = 1$ keV) and coronal parameters as for the separate disc-corona shown in Fig. 4a (where $\Gamma = 2.3$, $kT_e = 10$ keV, implying $f \sim 0.5$ in the corona) and b (where $\Gamma = 2.3$, $kT_e = 100$ keV, implying $f \sim 0.3$ in the corona).

Fig. 6 illustrates the differences between the coupled and uncoupled coronae by showing the individual spectral components for a corona with $\Gamma = 2.3$, $kT_e = 10$ keV and $r_c/r_{\text{in}} = 3.3$. Both spectra have the same $\dot{M}_{\text{disc},\infty}$, and assume the same inner disc radius (so without the corona both would give the same disc temperature of $T_{\text{in}} = T_{\text{in}}^{\text{int}} = 1$ keV) but there is much less total power in the coupled disc-corona system. This is as expected, as there is the additional coronal emissivity in the uncoupled disc-corona model. More importantly, the low energy rollover in the spectrum which is used to indicate the seed photon temperature is much lower in the coupled disc-corona. The reason for this is *not* primarily due to the reduction in temperature of the inner accretion flow under the corona. This is only a factor $(1-f)^{1/4}$ lower than $T_{\text{in}}^{\text{int}}$ i.e. 0.85 keV, so the low energy rollover in the Comptonised spectra is *not* significantly smaller ($4kT_{\text{in}}=3.4$ keV as opposed to 4 keV; KD04, magenta line). The major reason for the lower energy rollover in the total temperature is the reduction in *emissivity* of the inner disc in the coupled corona system. The dotted blue lines show the intrinsic inner disc emission, while the solid blue lines show the emergent, uncomptonised disc emission. The intrinsic disc emission is a factor $(1-f)$ weaker in the coupled disc-corona, so the Comptonised spectrum is also a factor $(1-f)$ weaker. A standard emissivity DISKBB has maximum luminosity from the inner disc components, hence the Comptonised emission (with its high seed photon rollover temperature) is generally *dominant*. For the coupled disc-corona, the reduction in emissivity under the corona means that the luminosity of the corona can be *less* than the luminosity of the outer disc. The Comptonised emission in the coupled system still contains a fairly high seed photon rollover ($(1-f)^{1/4}T_{\text{in}}^{\text{int}}$), but this can be masked by the much lower temperature rollover from the *outer* disc emission at $\sim T_{\text{in}}(r_c/r_{\text{in}})^{-3/4} \sim 0.4$ keV. The major effect of the coupled energetics is to decrease the fraction

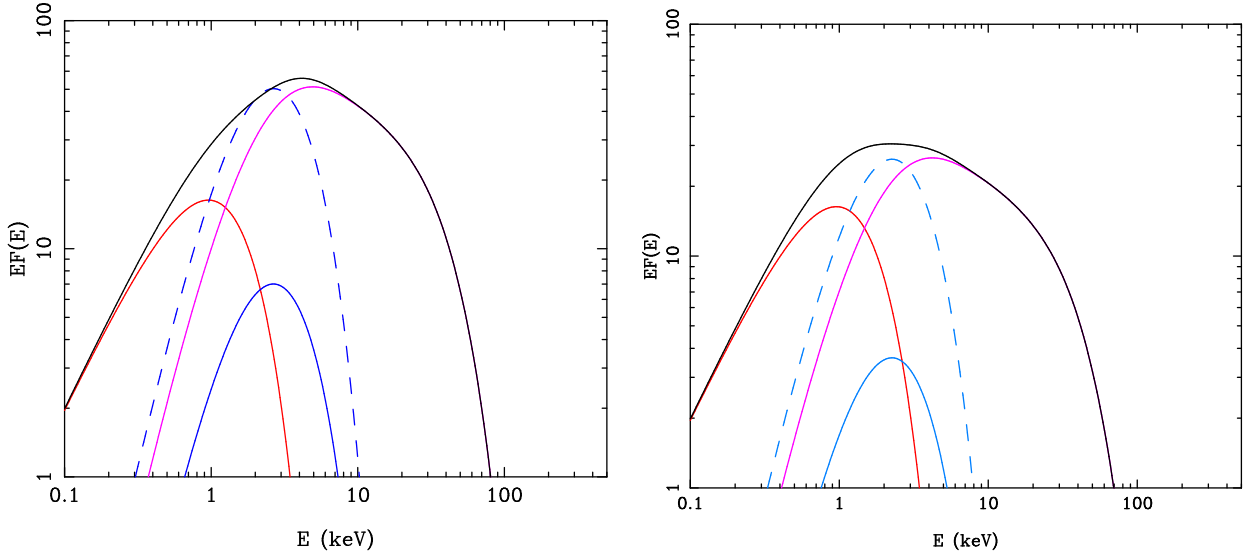


Figure 6. The model spectra for $\Gamma = 2.3$ and $kT_e = 10$ keV for $r_c/r_{in} = 3.3$. The total spectrum (black) is the sum of the contribution from the outer disc (red), uncomptonised inner disc (blue line), and comptonised emission (magenta). The dashed blue line shows the intrinsic (before comptonisation) inner disc emission. The left panel shows the uncoupled disc corona, while the right panel shows the coupled system. There is a marked decrease in luminosity in the coupled system due to the assumed emissivity (compare the right hand panels of Fig. 1b and c), but more importantly there is also a marked decrease in the low energy rollover seen in this spectrum. This is mostly due to the decrease in emissivity of the inner disc emission. This lowers the normalisation of the comptonised spectrum, so increasing the relative contribution of the low temperature, outer disc.

of energy emitted in the inner disc-corona, so enhancing the relative importance of the cooler, outer disc emission.

6.2 Data Fitting

We refit the data with this coupled disc-corona model, in which the disc emissivity *changes* from that of a standard disc. Again we use all 5 different descriptions of reflection to quantify the effect of systematic uncertainties in spectral modelling. Details of the fits to the data are given in Table 3, and again the models give equally as good a description of the data as either the uncoupled inner disc/slab corona (§ 5), or the continuous disc/corona system (§ 4).

The most obvious change from the coupled energetics is that the inferred inner disc radius is much smaller than in the previous fits. This is due to the same combination of two effects as given above (§ 6.1) i.e. firstly and most importantly the increased relative strength of the low temperature emission from the outer (unComptonised) disc, and secondly the slight reduction in temperature of the inner disc due to the energy drained from it to power the corona. The right hand panel of Fig. ?? shows the the derived luminosity and temperature of the disc *without* its corona, T_{in}^{int} , compared to the high/soft state luminosity-temperature data. The VHS points now lie much closer to those from the disc dominated states than before (left and middle panels of Fig. ??) though formally the statistical uncertainties show that the 20 % increase in disc radius in the VHS is significant (assuming a constant colour temperature correction). However, this is probably completely compatible with a constant disc radius given the systematic modelling uncertainties e.g. our assumptions about the shape of the corona (slab, with constant τ and T_e), the form of disc-corona coupling (all \dot{M}

through the disc, as opposed to some fraction of the accretion also taking place via the corona) and neglect of self-consistent reprocessing of the illuminating coronal flux by the disc.

7 SUMMARY OF SPECTRAL FITS

The VHS spectra seen in some high luminosity Galactic black holes are plainly strongly affected by Compton scattering. The most extreme VHS spectra no longer have a clear disc component, separate from the Compton scattered flux, but instead show a smooth continuum shape. This shows that the radii which produce the majority of the disc luminosity must be covered by optically thick material. However, even though the disc is hidden by this material, the inferred intrinsic disc luminosity and temperature can be estimated from broad bandpass spectra. The temperature can be determined from the low energy rollover in the Compton scattered spectrum, while the disc luminosity is related to the Compton scattered luminosity simply through the energy boost from Comptonisation. These VHS spectra are generally steep ($\Gamma > 2$) so the energy boost is not large.

However, to *robustly* constrain such spectra requires broad bandpass data, where the low energy rollover and all the thermal Comptonisation is covered by the observations. We use the two simultaneous ASCA-RXTE (0.7–200 keV) observations of the extremely Comptonised VHS spectra from XTE J1550 – 564 to investigate the intrinsic disc emission. As shown by KD04, this emission is *not* consistent with that seen in the disc dominated state from the same object. The temperature is much lower than that seen during the disc dominated states of the same luminosity. We

build a simple model of a slab corona over a disc to show that this conclusion holds irrespective of whether the corona covers the whole disc, or only the inner portion. The data strongly require that either the disc radius has increased, or the disc colour temperature correction has decreased, or the disc emissivity has decreased (or some combination of all three).

It seems highly unlikely that the colour temperature correction should decrease - the effects of irradiation and/or conduction would more naturally give an *increase* in surface temperature. Thus the possibilities reduce to a larger (by a factor 2) inner disc radius with standard emissivity, or a decrease in inner disc emissivity for a constant disc inner radius, or both (factor 1.2 increase in disc inner radius for the coupled disc-corona emissivity described above). We sketch each of these possible VHS geometries in Fig. 7a-c, respectively. If the disc does truncate, the accretion flow should still extend down to the last stable orbit unless there is a powerful outflow (wind/jet) at this point. Thus we show a continuous corona inward of the truncated disc as being the likely geometry in Figs.7a and c.

The one common denominator for *all* the geometries in Figs.7 is that the disc is *strongly* affected by the Comptonising corona. The coronal flow is *not* some separate phase of accreting material, e.g. a low angular momentum flow. Instead it *must* couple in some way to the disc.

8 ADDITIONAL CONSTRAINTS FROM THE DATA

However, there is additional information in the spectral and variability properties of these data which can give further constraints on the geometry. Firstly, the overall shape of the Comptonised spectrum is steep, so the average energy gain is rather small. This means that the seed photon luminosity is similar to the luminosity emitted by the electrons i.e. to the heating rate of the electrons. This is easy to arrange in the corona over the disc since the disc provides copious seed photons. However, it is much more difficult in the geometry of Fig. 7a, with the suggested continuation of the corona over a large range (factor 2) in radius down to the last stable orbit. The majority of the gravitational potential energy is dissipated in a region where there is no disc underneath, so the only seed photons for Compton cooling are a small fraction of those from the disc at larger radii. The combination of less Compton cooling and more electron heating would surely drive the coronal temperature to much higher values, leading to a much harder spectrum (as in the low/hard state). The smaller disc truncation implied by the geometry of Fig. 7c is much less of a problem, as the inner coronal flow is much smaller, so is energetically much less important.

Secondly, the changing frequencies of the type-C QPO's seen in the strongly Comptonised VHS data indicate that there is some change in characteristic radius picked out by the variability, and that this radius decreases with decreasing strength of Comptonisation in the spectrum (e.g. di Matteo & Psaltis 1999). In the specific relativistic precession model (Stella, Vietri & Morsink 1999), the low frequency QPO is formed from Lens-Thirring precession of vertical perturbations of the innermost edge of the disc and

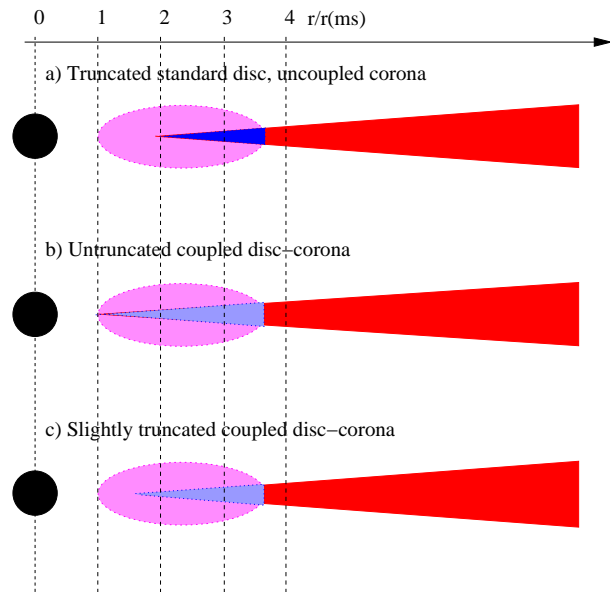


Figure 7. Possible geometries for the VHS, with radii for the disc and corona in a) and c) taken from the average of the Xi1, Xi2 and Xi3 model fits to the spectrum after the peak with DKBBTH (Table 2) and DKBBFTH (Table 3), respectively.

$\nu_{QPO} \propto r^{-0.33}$. The strongest low frequency QPOs (Type-C) are at 2.38 Hz and 3.90 Hz for the 1st and 2nd observations respectively, while in the weak VHS data, these are found at 5.9–6.5 Hz as Type-B QPOs (Remillard et al. 2002). The ratio of QPO frequencies between those seen in these strong VHS, and the most weakly Comptonised VHS is 2.6 and 1.6 implying a change in radius in the relativistic precession of about a factor 1.4 and 1.2 for the 1st and 2nd data set, respectively, assuming that the weakly Comptonised VHS has a disc which extends down to the last stable orbit (KD04). These estimates from the QPO's are startlingly close to the radii derived from our coupled disc-coronal fits, which imply a disc inner radius of $\sim 1.35 - 1.1 \times$ and $1.3 - 1.1 \times$ that inferred from the high/soft state data.

Conversely, the *changing* QPO frequency is a problem for the *constant* inner disc radius of Fig. 7b. Instead, the radius picked out by the QPO would have to be associated with a changing coronal radius rather than the inner disc itself. This has some advantages as the QPO is clearly associated with the *corona* rather than the disc (e.g. Gilfanov, Revnivtsev, & Molkov 2003), though it also seems likely that the outer coronal radius is related in some way to the inner radius of the disc (e.g. Churazov, Gilfanov & Revnivtsev 2001).

9 CONCLUSIONS

While all the geometries of Fig. 7 can explain the observed disc luminosity and temperature, we marginally favour that of Fig. 7c (slightly truncated disc, overlaid by an inner disc corona whose energetics are coupled to that of the disc) as this can consistently explain the QPO frequency as well. However, there is no clear consensus on models of QPO formation, so this cannot as yet give unambiguous information

on disc radii. Also, the derived slight truncation of the inner disc is very dependent on our very specific model for the coupled disc-corona. The disc area inferred from these strongly Comptonised VHS spectra can almost certainly be made to be completely consistent with that seen in the disc dominated states using slightly different coupling of the disc-corona system e.g. if some fraction of the accreting mass goes through the corona as well as some fraction of the power, or if the geometry of the corona is more quasi-spherical than slab-like. Thus Fig. 7b, where the disc area (though not its properties!) is unchanged from the disc dominated states is also consistent with the spectra, though this leaves the QPO's as an open question. Conversely, a large truncation radius with continuous corona (Fig. 7a) is ruled out by the steep Comptonised spectrum seen.

However, we stress that irrespective of the specific model, the strong Comptonisation seen in these very high state data clearly requires that the underlying disc properties are rather different to those of a disc without a corona. Unsurprisingly, the data require that the disc structure *changes* in response to whatever changing dissipation mode powers the growth of the coronal structure.

We also stress that these VHS spectra are very similar to those seen from several ULX in terms of having a very low apparent disc temperature for their luminosity. This has been interpreted as evidence for intermediate mass black holes in the ULX, of order $1000M_{\odot}$ (Miller, Fabian & Miller 2004). Obviously this is not an option in XTE J1550 – 564, where the black hole mass is constrained by dynamical studies to be a normal stellar remnant black hole mass of order $\sim 10M_{\odot}$ (Orosz et al 2002). We suggest that the same process, of a corona draining energy from the inner disc, may be operating in these ULX. Many of these would then be compatible with fairly normal binary systems, where the black hole mass is at the upper end of that which can reasonably form from models of stellar collapse (typically $30M_{\odot}$ or up to $\sim 80M_{\odot}$ from recent calculations; Belczynski et al. 2004) accreting at high mass accretion rates (0.1–few times the Eddington limit). We will explore this possibility in depth in a subsequent paper.

10 ACKNOWLEDGEMENTS

The present work is supported in part by JSPS grant of No.13304014 and No.14079101. CD thanks ISAS and RIKEiN for their hospitality during visits at which this work was carried out. AK is supported by special postdoctoral researchers program in RIKEN.

REFERENCES

Agol E., Krolik J. H., 2000, ApJ, 528, 161
 Ballantyne D. R., Ross R. R., Fabian A. C., MNRAS, 2001, MNRAS, 327, 10
 Belczynski K., Sadowski A., Rasio F. A., 2004, ApJ, 611, 1068
 Churazov E., Gilfanov M., Revnivtsev M., 2001, MNRAS, 321, 759
 di Matteo T., Psaltis D., 1999, ApJ, 526, 101
 Davis S. W., Blaes O. M., Hubeny I., Turner N. J., 2005, ApJ, 621, 372
 Done C., Gierliński M., 2003, MNRAS, 342, 1041

Done C., Madejski G. M., Zycki P. T., 2000, ApJ, 536, 213
 Done C., Zycki P., Smith D. A., 2002, MNRAS, 331, 453
 Ebisawa K. et al, 1994, PASJ, 46, 375
 Gierliński M., Done C. 2003, MNRAS, 342, 1083
 Gierliński M., Done C. 2004, MNRAS, 347, 885 (GD04)
 Gilfanov M., Revnivtsev M., Molkov S., 2003, A&A, 410, 217
 Hunstead R., McIntyre V., Lovell J., Reynolds J., Tzioumis T., & Wu, K. 2001, AP&SS, 276, 45
 Haardt F., Maraschi L. 1993, ApJ, 413, 507
 Kubota A., et al , 1998, PASJ, 50, 667
 Kubota A., Done C., 2004, MNRAS, 353, 980 (KD04)
 Kubota A., Makishima K., Ebisawa K., 2001, ApJ, 560, L147
 Kubota A., Makishima K., 2004, ApJ, 601, 428
 Makishima K., et al 1996, PASJ, 48, 171
 McClintock J. E., Remillard R. A. 2003, in Compact Stellar X-ray Sources, eds. Lewin W. H. G., & van der Klis, M., (Cambridge University Press, Cambridge), in press (astro-ph/0306213)
 Merloni A., Fabian A. C., Ross R. R., 2000, MNRAS, 313, 193
 Miller J. M., Fabian A. C., Miller M. C., 2004, ApJ, 614, 117
 Mitsuda K., et al 1984, PASJ, 36, 741
 Miyamoto S., Kimura K., Kitamoto S., Dotani T., Ebisawa K. 1991, ApJ, 383, 784
 Morrison R., McCammon D., 1983, ApJ, 270, 119
 Narayan, R., Yi, I. 1995, ApJ, 452, 710
 Orosz J. A. et al 2002, ApJ, 568, 845
 Pozdniakov L. A., Sobol I. M., Siuniaeov R. A. 1983, ASPR, 2, 189
 Remillard R. A., Sobczak G. J., Muno M. P., McClintock J. E., 2002, ApJ, 564, 962
 Ross R. R., Fabian A. C., Young A. J., 1999, 306, 461
 Shakura N., Sunyaev R., 1973, A&A, 24, 337
 Stella L., Mario V., Morsink S. M., 1999, ApJ. 524, L63
 Svensson R., Zdziarski A. A., 1994, 436, 599
 Tanaka Y., & Lewin W. H. G. 1995, in X-ray Binaries, eds. Lewin W. H. G., van Paradijs J. and van den Heuvel W. P. J., (Cambridge University Press, Cambridge), p126
 van der Klis M., 2004, in Compact Stellar X-ray Sources, eds. Lewin W. H. G., & van der Klis, M., (Cambridge University Press, Cambridge), in press (astro-ph/0410551)
 van der Klis M., 2000, ARA&A, 38, 717
 Zdziarski A. A., Johnson W. N., Magdziarz P., 1996, MNRAS, 283, 193
 Zycki, P. T., Done, C. & Smith, D. A., 1998, ApJ, 496, 25
 Zycki, P. T., Done, C. & Smith, D. A., 1999, MNRAS, 305, 231